Pergamon

0301-9322(94)E0030-M

*Int. J. Multiphase Flow* Vol. 20, No. 5, pp. 865–884, 1994

0301-9322/94 $7.00 + 0.00

# DUAL PRESSURE DROP METERING OF GAS–LIQUID MIXTURE FLOWS

M. R. DAVIS[1] and D. WANG[2]

[1]Department of Civil & Mechanical Engineering, University of Tasmania, G.P.O. Box 252C, Hobart 7001, Australia

[2]Department of Hydraulic Engineering, Wuhan University of Hydraulic and Electric Engineering, People's Republic of China

*(Received 30 June 1993; in revised form 4 April 1994)*

**Abstract**—The measurement of the two overall mass flow rates in a two-phase, gas–liquid pipeline is considered on the basis of dual pressure differential measurements for a combined contraction–frictional pipe type of flow meter. In particular the occurrence of compressible flow effects is established as an appropriate basis in such a metering arrangement for creating conditions where the two detected pressure differentials are not universally proportional. Under such conditions metering of the two flows in terms of the observed pressure differentials becomes practicable. The experiments generally conform with the predictions of a one-dimensional non-slip homogeneous flow model, and the correlation of wall friction factors with Reynolds number for gas–liquid two-phase pipe flow. The correlations of the velocity coefficients of abrupt and conical nozzles with void fraction have been obtained and incorporated in the analytical model for the flow meter. Whilst the practicability of such metering of two-phase flows is clearly demonstrated, application of the method would require careful calibration to allow for the influence of nozzle coefficient, pipe Reynolds number and void fraction upon the one-dimensional compressible flow equations through wall friction factor and interphase slip effects.

*Key Words:* two-phase flow, gas–liquid mixtures, flow metering, pipelines

## 1. INTRODUCTION

In this paper the establishment of a practicable basis for the measurement of two-phase (gas–liquid) volumetric flow rates in pipelines in terms of appropriate overall pressure drops is considered. In essence, it is necessary to determine the conditions for which the measurement of two system pressure differentials makes it possible to determine the two volumetric flow rates separately. The measurement of two pressure differentials will not always make this possible, since at relatively low flow velocities the mixture density may be virtually constant with the consequence that any two system pressure differentials governed by flow-induced pressure coefficients will maintain a constant ratio of one relative to the other and thereby preclude the use of the two observed values to solve separately for the two unknown flow rates. Couet *et al.* (1989) have approached this problem by making use of the gravitational forces acting for vertical flow through a nozzle of appreciable length. In a sense, this corresponds to the direct determination of mixture gas content or void fraction in terms of the gravitational pressure drop with height when combined with the usual reduction of pressure through a nozzle and its dependence upon mass flow rate. In the present work a different approach is adopted which involves the principles of compressible flow of gas–liquid mixtures in nozzles and in pipes with wall friction. Under compressible two-phase conditions, the pressure drop through a nozzle and in a pipe are no longer directly proportional, and it will be shown that this gives rise to the potential for separate determination of the two-phase volumetric flow rates from two observed pressure drops.

The analysis to be considered applies to gas–liquid mixture flows which are well mixed and bubbly. For such flows relative motion between the phases is generally small and the slip ratio is not greatly different from unity (Herringe & Davis 1978). In the analysis to be given here unity slip ratio will therefore be assumed, although it is possible to extend the method to cases of significant, known slip ratio.

Compressible gas–liquid mixture flows in contracting nozzles have been observed and analysed in detail by Thang & Davis (1979, 1981). The action of the contracting nozzle section is to somewhat increase bubble size, but provided the contraction is not too sharp or rapid, substantial relative motion between the phases does not arise. The pressure distributions along the nozzle axis were shown to be characterized in form by the void fraction at the nozzle throat, a critical point where the flow can be choked. These distributions show that larger normalized pressure ratios occur in the nozzle as the critical point void fraction decreases. As with compressible gas flow, the flows can only accelerate to high velocity in a convergent–divergent nozzle. Compressible flow and shock wave effects have been investigated by Campbell & Pitcher (1958), van Wijngaarden (1970) and Tangren *et al.* (1949).

Frictional flow of gas–liquid mixtures in a pipe also shows the characteristics of compressible flow with acceleration towards a critical or choking point at the pipe end being induced by the reduction of mixture density associated with pressure reduction (Huey & Bryant 1967; Davis 1974). Once again the characteristic form of the normalized pressure distribution with normalized distance along the pipe axis is determined by the critical point void fraction, with steeper pressure gradients occurring at lower critical point void fractions.

In the work to be described, the overall pressure ratios for flow with sudden and gradual contracting nozzles and along a pipe with wall friction will first be considered. Finally the combination of a gradual contracting nozzle and pipe in series and a sudden contraction nozzle and pipe in series will be analysed respectively and the potential of such combinations for determination of the flow rates of the two phases assessed. In particular, it is necessary to consider flow conditions, nozzle area contraction ratios and lengths of pipe which in combination will make it possible for the two flow rates to be resolved separately. Figure 1 illustrates the general layout of the proposed flow meter in which pressures, measured at the inlet and throat of the contraction and at the exit from the parallel pipe section, form the basis of flow metering of the two phases. It should be noted that real flow correction factors are introduced here, and that the performance of a real metering system depends on such effects not being influenced significantly by details of total system layout.

## 2. FLOW THROUGH A CONTRACTING NOZZLE

### *2.1. Density and void fraction of a gas–liquid mixture*

Gas–liquid mixtures experience close thermal contact between the two phases under conditions of turbulent, bubbly flow. A consequent expansion of the gas phase takes place isothermally as the mixture quality for bubbly flow is generally quite small. Since the liquid density is virtually constant, this leads to the mixture average density $\rho_m$ being given by

$$\rho_m = (1-\epsilon)\rho_L + \epsilon\rho_G = \rho_{m0}/(1-\epsilon_0+\epsilon_0 p_0/p) \qquad [1]$$

where suffix L and G denote liquid and gas, $\epsilon$ is the average local void fraction and $p$ the mixture pressure. Suffix zero denotes a reference condition at a convenient position along the flow direction. It follows that the local average mixture void fraction is given by

$$\epsilon = \epsilon_0 p_0/(p(1-\epsilon_0+\epsilon_0 p_0/p)) \qquad [2]$$

It should be noted that the gas density ($\rho_G$) is very much smaller than the liquid density ($\rho_L$) for the conditions investigated here (i.e. less than 1%).

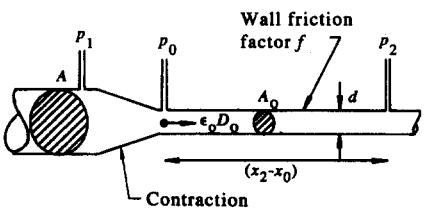


Figure 1. General configuration of a contraction–pipe two-phase flow meter.

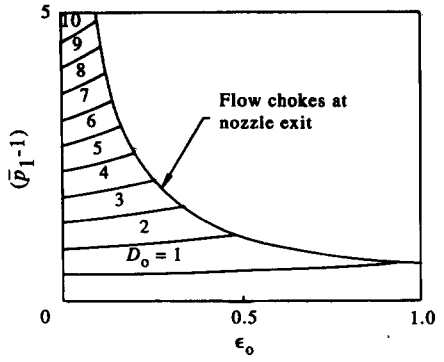


Figure 2. Normalized pressure differential across a contraction of area ratio 2.25 for various throat void fractions and normalized momentum flux parameters [5].

### *2.2. Ideal nozzle flow model*

Flow through a contracting nozzle is governed by continuity and momentum balance equations. Neglecting gravitational terms for nozzles which are horizontally oriented (or of a relatively small vertical extent if mounted vertically) and nozzle frictional losses, these equations are

$$\rho_m u_m A = \rho_{m0} u_0 A_0 \quad [3]$$

and

$$\rho_m u_m (du_m/dx) = -(dp/dx) \quad [4]$$

where $u_m$ is the average mixture velocity, $x$ is the distance along the flow direction and $A$ is the flow cross-sectional area. Combination with the mixture density equation [1], integration along the flow direction and elimination of the local velocity $u_m$ with the continuity [3], leads to [4] being re-arranged in the general form

$$(D_0/2)((1 - \epsilon_0 + \epsilon_0 p_0/p_1)^2 (A_0 A)^2 - 1) = (1 - \epsilon_0)(1 - p_1/p_0) - \epsilon_0 \log_e(p_1/p_0) \quad [5]$$

where the flow dynamic pressure term is $D_0 = \rho_{m0} u_{m0}^2 / p_0$. This parameter $D_0$ represents the momentum flux density at the reference position normalized in terms of the pressure at that position.

If the reference position is chosen to be the throat or outlet section of the contracting nozzle, then [5] shows how the pressure ratio across the contracting nozzle ($p_1/p_0$) varies with the two parameters $\epsilon_0$ and $D_0$ for a given area contraction ratio $A_0/A$. This relationship is illustrated in Figure 2, which demonstrates that the normalized nozzle pressure differential is determined primarily by the momentum flux parameter $D_0$ and to a much lesser extent by the flow void fraction ($\epsilon_0$). For small values of $D_0$ the pressure ratio becomes almost independent of void fraction since the mixture is then nearly incompressible. The pressure ratio is given for small $D_0$ by the simple incompressible value, which is then independent of $\epsilon_0$,

$$p/p_0 = 1 + D_0(1 - (A_0/A)^2)/2 \quad [6]$$

The pressure ratio is limited by the occurrence of choking at the nozzle throat. It has been shown by Thang & Davis (1981) that this occurs when $\epsilon_0 D_0 = 1$, since the effective Mach number in a gas–liquid homogeneous mixture flow is $(\epsilon D)^{1/2}$, as discussed in detail by Thang & Davis (1981). As shown in figure 2 the critical pressure ratio at which the nozzle chokes increases with reducing void fraction. Although it can be seen that the nozzle pressure ratio is dependent upon void fraction when $D_0$ is not small and the flow is then compressible and may approach choking at the throat, it is also evident that the nozzle pressure ratio is not extremely sensitive to void fraction for any value of $D_0$. As will be seen later this relative insensitivity of pressure ratio to void fraction for the contracting nozzle contributes usefully to the potential for metering two-phase flow rates by a combined contraction–pipe flow meter.

Experimental measurements of the pressure ratio across a contracting conical nozzle and an abrupt contraction nozzle are shown in figure 3 where they are compared with the values predicted

from [5] in terms of the known mixture conditions at the nozzle throat. These results are based on data obtained as described in section 5 using an air–water system with flow through a horizontal contraction. It can be seen from figure 3 that there is moderately good agreement between measured and predicted pressure ratios for a gradually contracting nozzle, although the measured pressure ratios tend to be somewhat smaller. Essentially this is because the real nozzles have discharge coefficients less than unity, particularly the abrupt nozzle, whereas [5] is based on ideal nozzle behaviour. This would be due to modest slip at the nozzle throat of the conical contraction since the consequence of such slip is for the liquid phase to move more slowly at the throat than the overall average mixture velocity and hence to reduce the pressure drop which actually occurs since the actual flow momentum flux is dominantly associated with the liquid phase. A more detailed investigation of flow structure in venturi nozzles using voidage probes (Thang & Davis 1981) supports this argument as larger slip was observed at the throat for more rapid contractions. The contraction for which the data of figure 3 were obtained would be expected to give rise to only modest velocity ratios of about 1.1 at the throat, this being close to the slip ratio also expected at the inlet to the contraction. The data of figure 3 were obtained using the same type of multi-jet mixer as that used by Thang & Davis (1981) so that generally similar inlet flows would be expected. It can also be seen from figure 3 that a difference between the measured and predicted pressure ratios for abrupt contractions is evident, and these observed results give pressure differences of only about 0.4 times the predicted pressure differences. This would mainly be due to flow separation due to the sudden change of cross section.

### *2.3. Real nozzle flow model*

Considering the losses due to the variation of cross-sectional area and the friction in the nozzle, the momentum balance equation [4] can be modified as

$$\rho_m u_m \frac{du_m}{dx} = -\left(\frac{dp}{dx} + \frac{4\tau_n}{d_n}\right) \qquad [7]$$

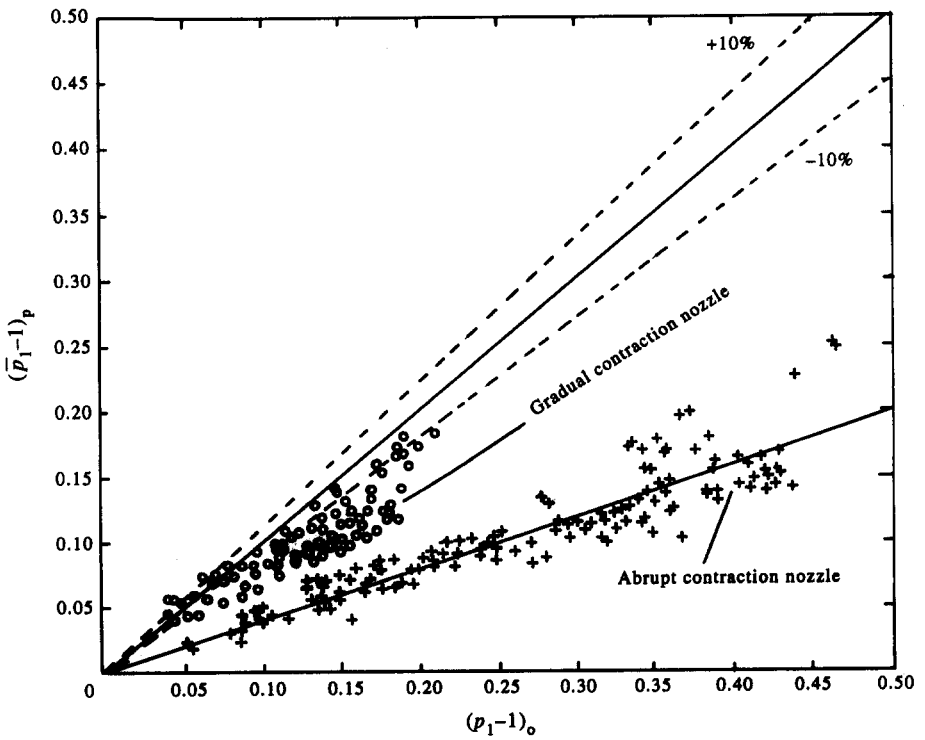


Figure 3. Comparison of observed pressure change $(\bar{p}_l - l)_0$ across a contraction with predicted change $(\bar{p}_l - l)_p$ for the homogeneous non-slip equation [5]. Contraction area ratio = 2.25, inlet diameter = 38.1 mm, axial length of conical contraction = 31 mm. Points, measured data, solid line with dashed range lines, predicted values ± 10% range [5].

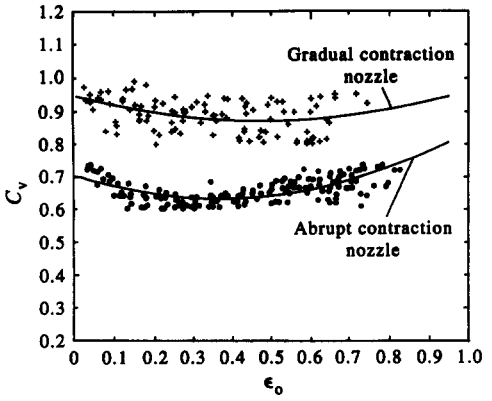


Figure 4. Variation of nozzle velocity coefficient with void fraction. (Geometry as for figure 3.)

where $\tau_n$ is defined as the sum of the shear stress between fluid and boundary and the interphase shear stress, and can be expressed as $\tau_n = k_n \rho_m u_m^2/2$, $k_n$ is a coefficient dependent on the configuration of the nozzle and the void fraction of mixture and $d_n$ is the diameter of nozzle outlet.

Combining [7] with the mixture density equation [1] and continuity equation [3], the expression for the dynamic head parameter $D_0'$ in real nozzle flow can be obtained and can be simplified as

$$D_0' = \phi_n^2 D_0 \qquad [8]$$

where $\phi_n$ is the velocity coefficient of the nozzle which will depend on the void fraction of the mixture and the configuration of nozzle, and can only be obtained from experimental data.

The value of $\phi_n$ obtained from gradual and abrupt contracting nozzles for different void fractions is shown in figure 4, and the correlation of $\phi_n$ with void fraction $\epsilon_0$ for an abrupt contracting nozzle of area ratio 2.3 is found to be

$$\phi_n = 0.571\epsilon_0^2 - 0.413\epsilon_0 + 0.702 \qquad [9]$$

For a gradually contracting nozzle of the same area ratio as the abrupt contracting nozzle, the correlation of $\phi_n$ with void fraction $\epsilon_0$ is as follows:

$$\phi_n = 0.95 - 0.328\epsilon_0 + 0.34\epsilon_0^2 \qquad [10]$$

From figure 4 it is found that when the void fraction approaches unity or zero the value of $\phi_n$ is similar to that obtained for single-phase flow. The maximum nozzle loss occurs when the void fraction is between 0.2 and 0.4. Equations [9] and [10] are shown by the solid lines in figure 4.

Substituting $D_0$ in [5] with [8] leads to [5] being rearranged in the general form for the pressure at section 1,

$$(D_0'/2)((1 - \epsilon_0 + \epsilon_0 p_0/p_1)^2(p_0/p_1)^2 - 1) = \phi_n^2[(1 - \epsilon_0)(1 - p_1/p_0) - \epsilon_0 \ln(p_1/p_0)] \qquad [11]$$

The values of the pressure ratio predicted from [11] and [9] and from [11] and [10] are compared with experimental measurements of the pressure ratio across an abrupt contracting nozzle and a gradual contracting nozzle as shown in figure 5. It can be seen that there is good agreement between measured and predicted pressure ratios for both gradual and abrupt contracting nozzles. It should be noted that due to the congestion of points on figure 5, some data values are not shown. The overall agreement of observed and predicted results is ensured by selection of the appropriate correction factor, but some scatter is still evident in the actual measurements.

## 3. PRESSURE DROP IN THE PIPE SECTION

The streamwise momentum balance equation for flow resisted by wall friction in the circular pipe section neglecting slip is

$$\tau_w + (d/4)(dp/dx) + (\rho_m u_m d/4)(du_m/dx) + \rho_m g d/4 = 0 \qquad [12]$$

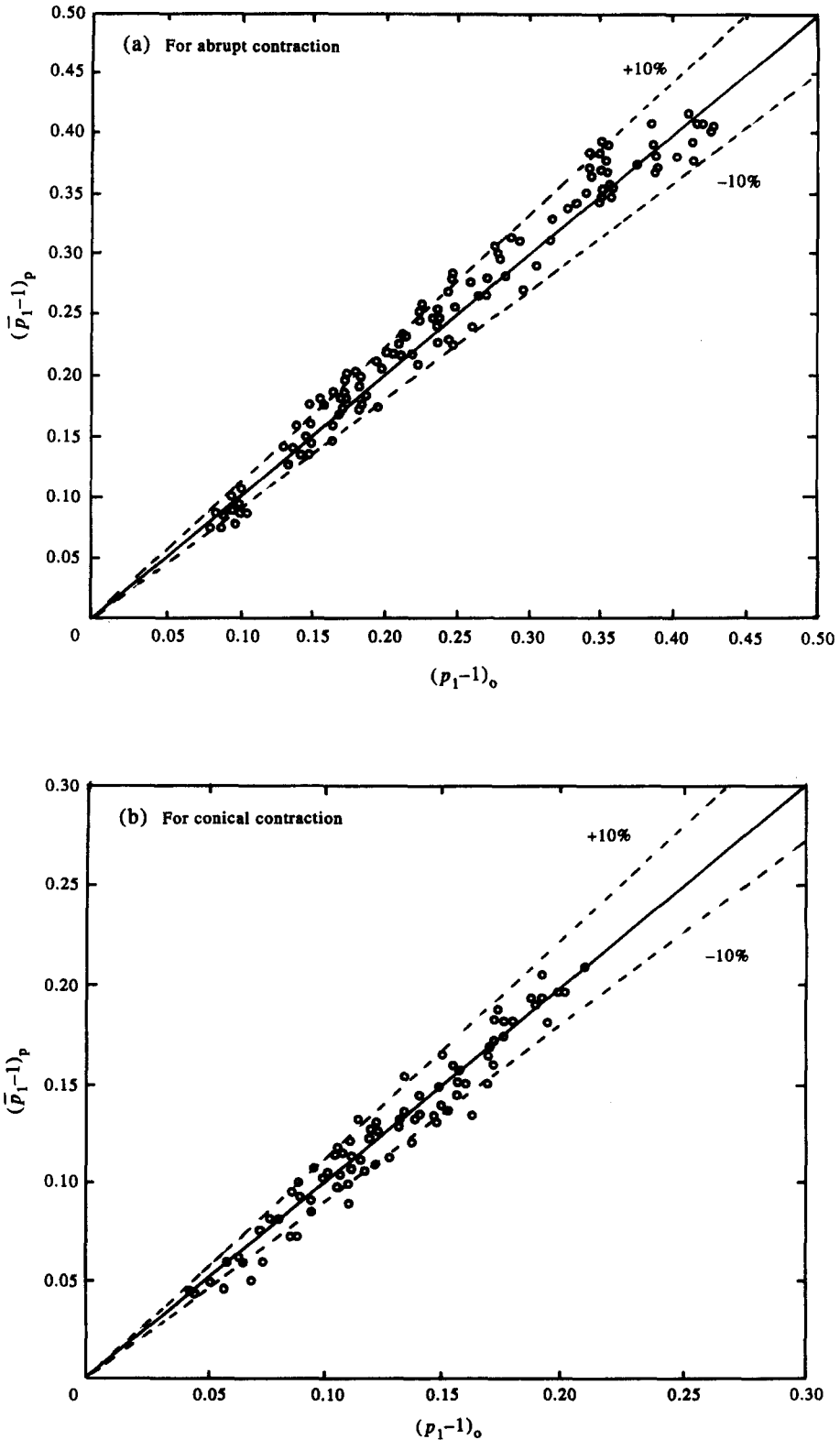


Figure 5. Comparison of observed pressure change $(\bar{p}_1 - l)_0$ across a contraction with predicted change $(\bar{p}_1 - l)_p$ for the homogeneous non-slip equation [11]. (a) For abrupt contraction; (b) for conical contraction. (Geometry as for figure 3.)

where $x$ denotes distance along the tube of diameter $d$, $u_m$ is the mixture velocity, $g$ is the component of gravitational acceleration along the pipe and the wall shear stress is $\tau_w$. The shear stress is related to the mixture conditions by a friction factor $f$ in the usual manner,

$$\tau_w = f\rho_m u_m^2/2 \quad [13]$$

Combining these equations, [7] can be integrated along the pipe length to obtain the streamwise distribution of pressure. Extending this integration over the pipe length between positions denoted by suffixes 0 and 2, we then have

$$f(x_0 - x_2)/d = a\{(\bar{p}_2 - 1) + (A/2)\log_e[(\bar{p}_2^2 + b\bar{p}_2 + c)/(1 + b + c)] + (B - bA/2)I + C\log_e \bar{p}_2\} \quad [14]$$

A full derivation of this equation is given by Davis (1974).

The six constants involved in this equation are expressed only in terms of conditions at the start of the pipe section (suffix zero)

$$a = (1 - \epsilon_0)/\{2D_0(1 - \epsilon_0)^2 + D_0/F_0 f\},$$
$$b = 4\epsilon_0 D_0 a$$
$$c = 2\epsilon_0^2 D_0 a/(1 - \epsilon_0),$$
$$A = \epsilon_0/(1 - \epsilon_0) - b - C$$
$$B = -\epsilon_0 D_0 - c - bC,$$
$$C = -\epsilon_0^2 D_0/[(1 - \epsilon_0)c]$$

and $I$ represents the result of integration as follows, if $c > b^2/4$

$$I = [1/(c - b^2/4)^{1/2}][\tan^{-1}\{(\bar{p}_2 + b/2)/(c - b^2/4)^{1/2}\} - \tan^{-1}\{(1 + b/2)/(c - b^2/4)^{1/2})\}]$$

or if $b^2/4 > c$ then

$$I = \{1/2(b^2/4 - c)^{1/2}\}\ln[((b^2/4 - c)^{1/2} - \bar{p}_2 - b/2)((b^2/4 - c)^{1/2} + 1 + b/2)/\{((b^2/4 - c)^{1/2} + \bar{p}_2 + b/2)((b^2/4 - c)^{1/2} - 1 - b/2)\}]$$

In these experiments $\bar{p}_2 = p_2/p_0$, the pressure ratio across the test length, whilst flow momentum flux and gravitational effects along the pipe are represented in the constants $D_0 = \rho_{m0}u_{m0}^2/p_0$ and $F_0 = u_{m0}^2/gd$. $u_{m0}$ is the average mixture velocity (total volumetric flow divided by pipe area) at the reference section denoted by suffix zero.

For specified conditions at the pipe entry in terms of void fraction ($\epsilon_0$), flow momentum flux ($D_0$) and gravitational force components along the pipe ($F_0$), [14] can be solved numerically for the pressure ratio ($p_2/p_0$) across the complete pipe section between the measuring points at sections 0 and 2 if the product of wall friction factor and normalized length ($f(x_2 - x_0)/d$) is known. The dependence of the overall pressure ratio upon the inlet conditions of voidage and momentum flux for a given constant wall friction factor is shown in figure 6. At low values of the momentum flux parameter ($D_0$) the flow at the inlet and along the whole pipe length is close to being incompressible and the pressure ratio is approximately proportional to $D_0$ and independent of inlet void fraction ($\epsilon_0$). However, as $D_0$ increases, so the Mach number at exit ($M_2 = \sqrt{\epsilon_2/D_2}$) also increases and the pressure ratio is then influenced by compressible flow effects. This is reflected by an increasing dependence of the pressure ratio upon inlet void fraction ($\epsilon_0$) as well as upon the momentum flux ($D_0$) evident in figure 6 for larger values of $D_0$. Ultimately the flow at section 2 reaches a critical condition and the pipe section is then choked. For any given conditions the values of $D_2$ and $\epsilon_2$ at the downstream section can be determined from the pressure ratio given by [14] and the inlet parameters using [2] to determine the void fraction and the definition of $D_2$ used in combination with the continuity of mass flux and [1] to give

$$D_2 = \frac{\rho_{m2}U_{m2}^2}{p_2} = D_0(1 - \epsilon_0 + \epsilon_0(p_0/p_2))(p_0/p_2) \quad [15]$$

Hence it is possible to determine when choking of the pipe occurs (i.e. when $\epsilon_2 D_2 = 1$) and to construct the limiting envelope for outlet choking of the pipe as shown in figure 6. It can thus be

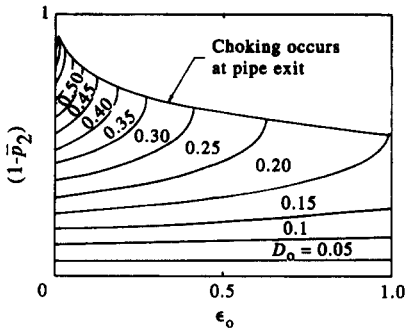


Figure 6. Normalized pressure differential over a pipe section for various inlet void fractions and normalized momentum flux parameters (pipe length = $l$, diameter = $d$, friction factor = $f$, [14]). ($fl/d = 0.6$; $1/F_0 f = 0$).

seen that it is necessary for the outlet flow conditions at section 2 to approach choking if a stronger variation of the overall pressure ratio with void fraction ($\epsilon_0$) is to be introduced.

Experimental observations of the pressure distribution along a circular pipe are shown in figure 7. It can be seen that for the flows for which choking occurs the pressure gradient becomes much steeper as the end position is approached. This is to be expected as the pressure gradient for a homogeneous flow should become infinite at the point of choking, the flow being similar to the Fanno type flow of a compressible gas in a tube.

Experimentally observed pressure distributions over known lengths of pipe can be used to determine the pipe friction factor from [14] in terms of the pressure ratio, known inlet conditions and pipe length. This calculation can be carried out over either a complete pipe length or over any intervening section. An extensive set of pressure measurements at the inlet, outlet and one intermediate pressure tapping were analysed on this basis for a variety of inlet flows. It was found that measurements of friction factor close to the pipe end become quite irregular if choking at the end occurred. It was concluded that, since the back pressure was appreciably lower than the pressure just inside the pipe for such tests, an expansion wave system had been set up within the flow at the pipe exit. Given that the flow was not perfectly uniform over the cross section, some effects of this expansion wave system would be expected to be experienced within the pipe itself, especially near the walls where the mixture void fraction is somewhat lower (see Herringe & Davis 1978) and the local pressure wave velocity higher therefore. However, provided local pressures were

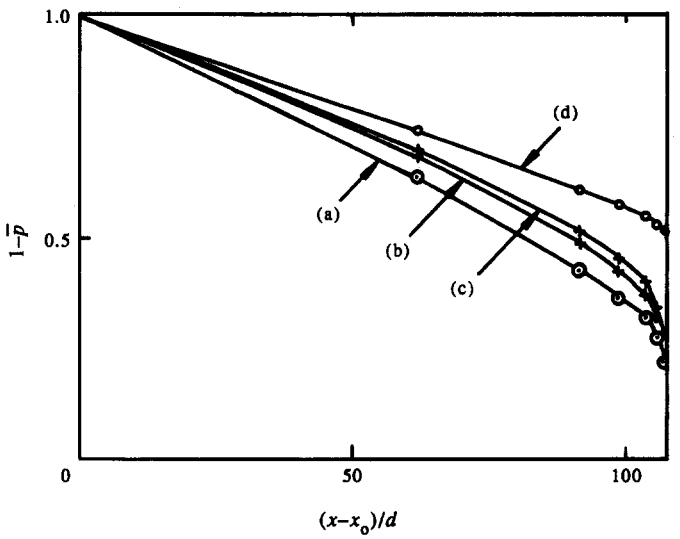


Figure 7. Observed pressure distributions along a horizontal pipe (pipe diameter = 25.4 mm). Inlet conditions: (a) $\epsilon_0 = 0.06$, $D_0 = 0.21$; (b) $\epsilon_0 = 0.15$, $D_0 = 0.15$; (c) $\epsilon_0 = 0.23$, $D_0 = 0.13$; (d) $\epsilon_0 = 0.29$, $D_0 = 0.10$. [Flows (a), (b) and (c) were choked, flow (d) was not.]

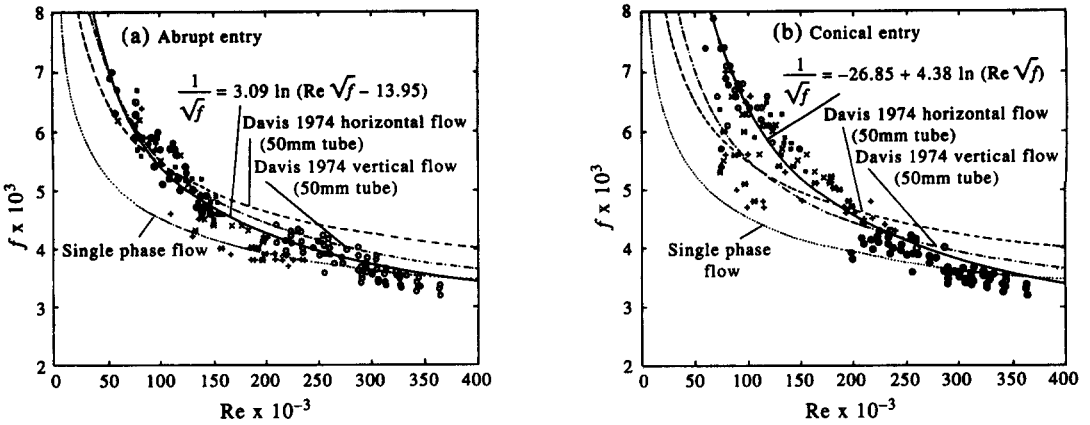


Figure 8. Variation of pipe friction factors from the observed pressure drop in a horizontal flow using [14]. (Pressure drop observed between $x_0/d = 0$ and $x_2/d = 110$, pipe diameter = 25.4 mm. Physical end of pipe at $x/d = 156$.) +, $\epsilon_0 < 0.25$; *, $0.25 \leqslant \epsilon_0 < 0.35$; ×, $0.35 \leqslant \epsilon_0 < 0.45$; $0.45 \leqslant \epsilon_0 < 0.55$; Ø, $0.55 \leqslant \epsilon_0 < 0.65$; ⊕, $0.65 \leqslant \epsilon_0 < 0.75$; •, $0.75 \leqslant \epsilon_0 < 0.85$; ○, Davis (1991) (25 mm tube). (a) Abrupt entry; (b) conical entry.

not measured within approximately five tube diameters of the exit it was found that consistent values of the wall friction factor were determined from the pressure data.

Average friction factors were calculated here from the pressure ratio observed over a length of 110 tube diameters with the downstream pressure tapping at a distance of 46 tube diameters ahead of a discharge elbow. Average wall friction factors were also calculated from observed pressure differentials observed over a length of 98.75 tube diameters (with downstream pressure tapping at a distance of 9.25 tube diameters from the outlet of tube) by Davis (1991). Both sets of data are shown in figure 8 as a function of the flow Reynolds number. The Reynolds number is calculated in terms of the mixture mass flow rate and liquid viscosity ($\mu_L$) since the shear stress at the wall is transmitted through a liquid layer close to the wall, $Re = \rho_m U_m d/\mu_L$. The Reynolds number remains constant along the pipe. It can be seen that there is a clear trend for the wall friction factor of the pipe to reduce regularly with increasing Reynolds number. The dependence of wall friction factor upon Reynolds number for an air–water mixture flow through the pipe with abrupt entry can be correlated as

$$\frac{1}{\sqrt{f}} = 3.09 \ln(Re\sqrt{f}) - 13.95 \qquad [16]$$

For an air–water mixture pipe flow with a conical contraction entry, the correlation was found to be

$$\frac{1}{\sqrt{f}} = 4.38 \ln(Re\sqrt{f}) - 26.85 \qquad [17]$$

The correlations above are compared with that proposed by Davis (1974) for horizontal and vertical water–air mixture flow, and the correlation proposed by Nikuradse for single-phase flow in figure 8(a) and (b). It can be seen that there is moderately good agreement between measured results from various experiments. The difference between present correlations and the correlation proposed by Davis (1974) would be due to the variation of flow pattern through the pipe due to the influence of the pipe contraction. This is immediately upstream of the pipe length in the present work, whereas the earlier experiments (Davis 1974) allowed a settling pipe length ahead of the test pipe length. However, in the present flow meter application, it is necessary for the nozzle to lead directly to the pipe length so that only three pressure measurement points are required. It can be concluded that the flow pattern at the entry of the pipe is influenced by the configuration of contraction in the present experiment. There is a significant influence of this on the pressure drop along the pipe, especially at low Reynolds number flow conditions, and therefore the contraction affects the correlation of wall friction factor with Reynolds number as shown by comparing figure 8(a) and (b) or [16] and [17].

## 4. COMBINED CONTRACTION–PIPE FLOW METER

Having demonstrated experimentally that bubbly flows (with void fractions between 0.05 and 0.8 approx.) conform to the general predictions of the one-dimensional flow equations for nozzles and pipes, the possibility of using a combined system for flow metering will be considered.

### *4.1. Performance prediction for ideal flow conditions*

It is first necessary to investigate the range of flow conditions over which a flow meter would allow resolution of the two flow rates and what type of design, in terms of contraction ratio of the nozzle and length of pipe section, will be optimal. At this stage, an ideal operation condition in which the wall friction factor of the pipe section is constant and the velocity coefficient of nozzle is unity is assumed in order to simplify the analysis.

The variation of predicted normalized pressure differentials for an ideal nozzle ($C_v = 1$) and pipe section is shown in figure 9 as a function of the momentum flux parameter ($D_0$) and void fraction ($\epsilon_0$) at the exit from the contraction and entry to the pipe section. Two system geometries are illustrated, corresponding broadly to a relatively large contraction ratio and short pipe length [figure 9(a)] and to a small contraction ratio and long pipe length [figure 9(b)]. These diagrams have been computed from [5] and [14] on the basis of a constant friction factor.

These results demonstrate that for compressible flow conditions (i.e. larger momentum flux parameter values) the influence of void fraction on the pipe section pressure differential clearly causes a spread of the constant void fraction curves over the pressure differential diagram. Thus a measurement of dual pressure differences in the higher range of $D_0$ above 0.3 typically would give rise to the ability to determine both $D_0$ and $\epsilon_0$ from the two pressure differentials over the nozzle and pipe sections. For small values of $D_0$ less than approx. 0.2 the constant void fraction curves converge and in this region it would not be practicable to discriminate both parameters ($\epsilon_0$ and $D_0$, and hence the flow rate of both phases) separately. Figure 9 also shows that the selection of system geometry is not critical insofar as the ability to determine both phase flow rates is concerned as comparable relative spreads of the constant void fraction curves occur in both cases illustrated. However, adjustments to the length of the pipe section and area ratio of the contraction will of course influence the relative magnitude of the range of pressure drop to be measured over each of the two measurement sections.

The effect of operating the flow meter in the horizontal position ($1/F_0 f = 0$) or in the vertical position with upward flow is also shown in figure 9(a)–(c). The influence of the gravitational term in the pipe section is to increase the pressure drop and thereby promote more rapid onset of choking. This therefore confines the operating range to lower values of the momentum parameter $D_0$, and has the effect of substantially diminishing the potential of the system for dual flow rate determination from dual pressure drop data since the spread of lines of constant void fraction over the measured parameter diagram is considerably reduced. It appears therefore that the veritical upward configuration is not suitable for the purpose of two-phase flow metering by use of the compressible characteristics. For vertically downward flow the effect of the gravitational terms in the pipe section is reversed, and as a consequence [figure 9(d)] the spread of constant voidage and momentum parameter lines over the range of measured pressure drops is more similar to that obtained in horizontal flow. Therefore vertically downward flow maintains the general suitability of the system for two-phase flow metering.

As the condition of choking is approached it can be seen that both lines of constant momentum flux and constant void fraction tend to give constant nozzle contraction pressure differentials whilst the pipe section pressure differential increases rapidly as choking is approached. Under these conditions, observation of the contraction section pressure drop alone indicates a unique pair of values of the void fraction and momentum flux parameter at the choking point, and the determination of these two parameters from the pipe section pressure drop as well would become of less importance. However, apart from the dominant influence of the nozzle pressure ratios for such conditions, voidage and momentum parameters could still be determined. For choked flows the determination of both $\epsilon_0$ and $D_0$ from the single observed pressure ratio in the nozzle section is possible since these two parameters are then directly related under the conditions of choking ($\epsilon_2 D_2 = 1$). We see that the most flexible operation of the dual pressure drop flow meter will occur

when the flow in the pipe and nozzle are appreciably compressible but without approaching choked conditions too closely in the measurement sections so that choking constraints are not introduced. This is consistent with avoidance of the effects of choking at the pipe end by ensuring that the downstream pressure measuring point is located some distance upstream of the physical end of the pipe as discussed in section 3.

### *4.2. The prediction of real operation conditions*

Operation of a combined contraction–pipe type of flow meter would actually be subject to the configuration of the contraction and the wall friction factor associated with momentum flux, void fraction and Reynolds number. The expression for the Reynolds number can be rearranged as

$$\mathrm{Re} = ((\rho_L(1-\epsilon) + \rho_G \epsilon)Dp)^{1/2} \cdot (d/\mu_L) \qquad [18]$$

where $d$ is the diameter of pipe or contraction outlet, $p$ is the pressure, $D$ is the momentum flux parameter, $\epsilon$ is the void fraction, $\mu_L$ is the liquid viscosity and $\rho_L$, $\rho_G$ are the densities of liquid and gas, respectively. This definition of Reynolds number is based on the conventional choice of

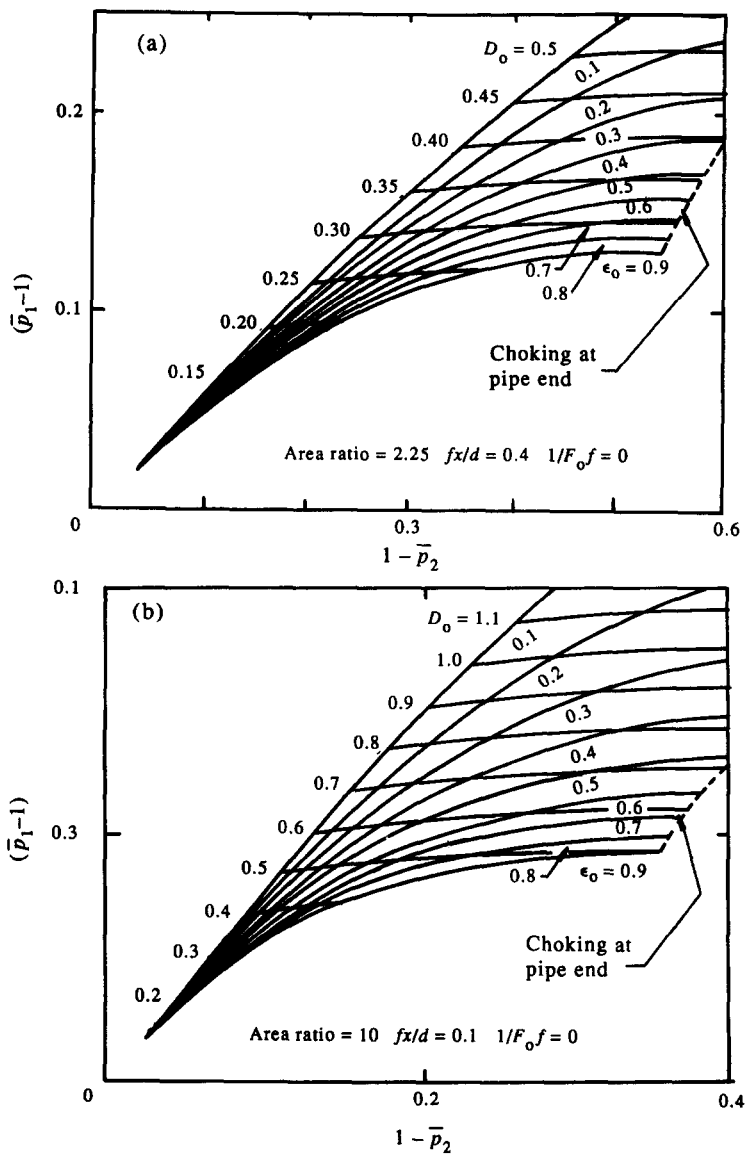


Fig. 9 (a) and (b). *Caption overleaf.*

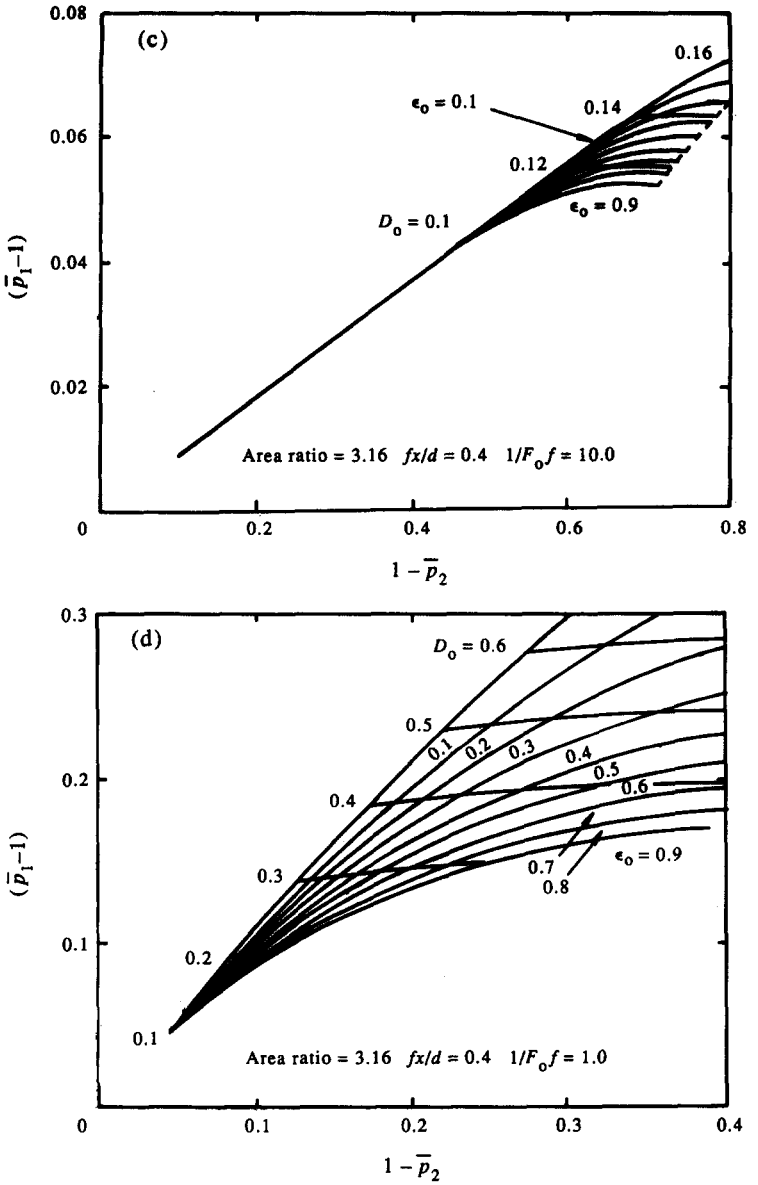


Fig. 9 (c) and (d)

Figure 9. Variation of normalized pressure differential across a series contraction and a pipe for an ideal homogeneous flow model. (Horizontal flow, $1/F_0f = 0$.) (a) Area ratio = 2.25, $fx/d = 0.4$, $1/F_0f = 0$; (b) area ratio = 10, $fx/d = 0.1$, $1/F_0f = 0$; (c) area ratio = 3.16, $fx/d = 0.4$, $1/F_0f = 10.0$; (d) area ratio = 3.16, $fx/d = 0.4$, $1/F_0f = -1.0$.

momentum flux and liquid viscosity as the relevant parameters as is used in the correlation of frictional data (Davis 1974).

If $\rho_G/\rho_L \cong 0$, then [17] becomes

$$\mathrm{Re} = \rho_L(1-\epsilon)U_m d/\mu_L \qquad [19]$$

It can be seen that for a given momentum flux parameter $D$ the Reynolds number will decrease with increase of void fraction from [18] and the wall friction factor will also increase from figure 8(a) and (b). If $\mathrm{Re} < 200 \times 10^3$, the influence of void fraction on wall friction factor will become much more important. This would have the effect of reducing the pipe section pressure ratios, especially at small values of the momentum flux parameter and deforming the constant void fraction curves in figure 9. For a given pressure differential, the corresponding value of the

parameter $D_0$ will be affected by the configuration of the contraction, which is represented here by the velocity coefficient of the contraction, and also by the flow pattern at the entry of the contraction.

Considering the factors discussed above, a real prediction model for a contraction pipe flow meter has been found, and the variation of normalized pressure differentials over the contraction and pipe section is shown in figure 10. These have been computed from this model by combining [11], [14] with [9], [16] or [10] and [17] for water and gas flow in the pipe of diameter 25.4 mm. Comparing figure 9 and figure 10, it can be seen that the influence of Reynolds number on the wall friction factor has broadened the measurement space between the different constant void fraction curves, especially for small values of momentum flux parameter $D_0$. This has made this type of flow meter more suitable for operation at small values of momentum flux parameter when void fraction is greater than 0.4. From figure 10 it can also be seen that the compressibility of the

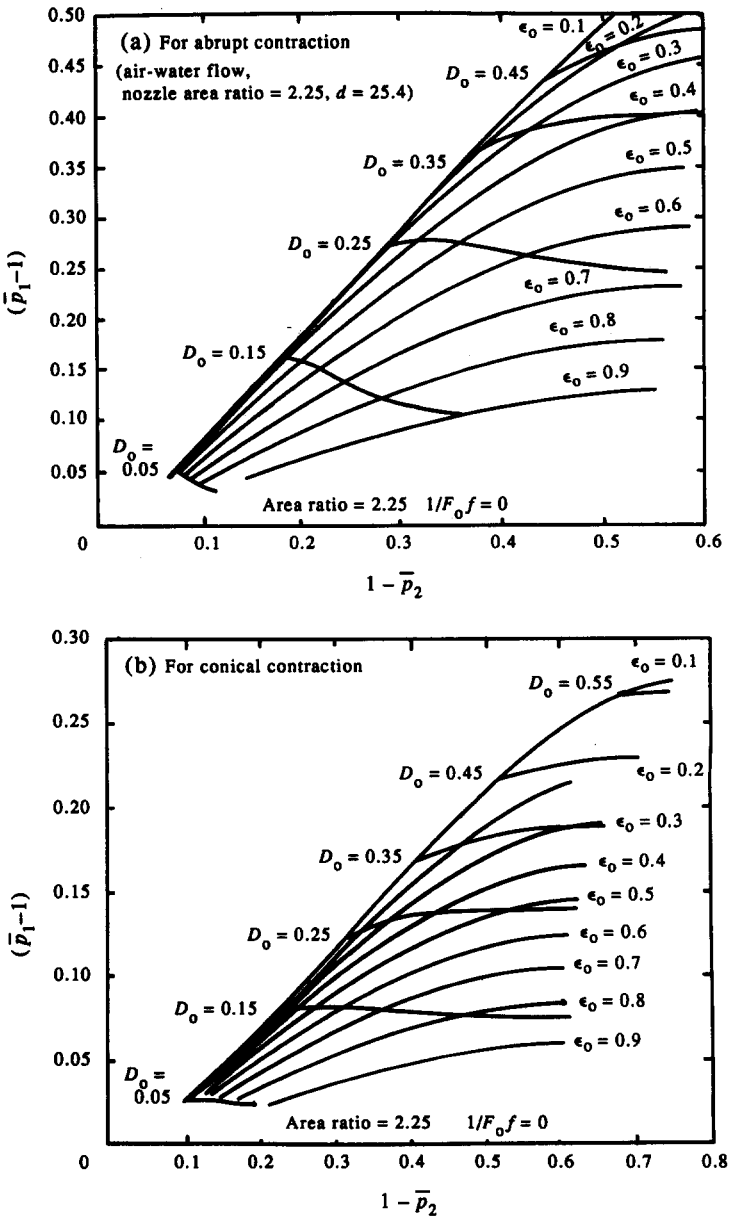


Figure 10. Variation of predicted normalized pressure differential across a series contraction and a pipe under real operating conditions. (a) For an abrupt contraction, area ratio = 2.25, $1/F_0 f = 0$; (b) for a conical contraction, area ratio = 2.25, $1/F_0 f = 0$ (air–water flow, nozzle area ratio = 2.25, $d = 25.4$ mm).

gas–liquid mixture is related to void fraction and momentum flux parameter, and the conditions for establishing compressible flow in the frictional pipe section correspond to a requirement that the mixture momentum flux $D_0$ at the pipe entry is approx. 0.35 if void fraction is greater than 0.1 so that the sensitivity of the dual pressure differential observations can reasonably be used to determine the void fraction and momentum flux parameter. However, by contrast to the ideal prediction model shown in figure 9, which is a general prediction model and independent of the properties of the mixture and pipe diameter, the results of the real prediction model can be obtained only for a specified pipe diameter and fluid due to the influence of Reynolds number on pipe diameter $d$ and fluid properties ($\rho_L$ and $\mu_L$). Figure 10 thus applies only for the flow of water–air mixtures through a pipe of diameter $d = 25.4$ mm. Application of these results to other working fluids would require careful review of the characteristics of the flow structure.

## 5. EXPERIMENTAL OBSERVATIONS WITH A COMBINED CONTRACTION–PIPE FLOW METER

The experimental observations were carried out using an air–water mixture in a horizontal flow system. The air–water mixture was formed by a conical multi-jet mixer of the type similar to that described by Herringe & Davis (1976). The mixing chamber was of overall length 0.42 m, and was in the form of a smooth conical contraction from the base plate of diameter 0.104 m to the outlet of diameter 0.0381 m, which was connected by a pipe of constant diameter 0.0381 m and of length 2.1 m to the entry of the contraction. Air from a compressor was injected through a central hole of diameter 0.0125 m in the base plate, and water through eight 0.011 m holes in the base plate on a 0.08 m diameter circle. The mixture flows from the outlet of the mixing chamber were of a turbulent, bubbly type, and remained relatively steady without any tendencies to form slugs or intermittent flow or to break down into annular patterns as determined from visual observation in the range of average void fractions extending from 0.2 to 0.75. This was a consequence of the relatively high flow velocity at which the compressible flow effects are achieved in this gas–liquid flow by the dual pressure differential type of flow meter. The precise extent of the bubbly flow regime is, of course, subject to uncertainty, and it appears therefore that the results of the present work may extend somewhat beyond the region of bubbly flow under some definitions. As far as the present work is concerned the question is really the range of conditions over which the homogeneous model provides a workable basis rather than what exactly constitutes bubbly flow. Two types of contractions, i.e. an abrupt contraction and a conical contraction, with the same area ratios were combined with the pipe in series and tested, respectively, as a combined contraction–pipe flow meter. The inlet of the contractions was 0.0381 m diameter, and the outlet of contraction and entry of the pipe was 0.0254 m diameter. The conical contraction had a length of 31 mm. The mixture flow from the mixing chamber passed through the combined contraction–pipe flow meter, the pipe length being 2.75 m, and then travelled an additional distance of 1.4 m through an elbow before discharging at a submerged end into a weir tank. Overall flow rates of the two-phase mixture were measured externally by means of a standard orifice for the inlet air and V notch weir for the water flow after separating outlet air from water. Experiments were conducted using smooth perspex tubes. The pressures at the inlet of contraction, throat and the outlet of the test pipe section were measured by oil-filled precision pressure gauges in order to eliminate fluctuations so that the dual pressure differentials could be determined. The pressure observed at the throat by a wall pressure tapping was also used to determine the volumetric flux of the mixture at that point neglecting slip between the two phases. Pressure tappings were made by drilling 1 mm flush holes through the top of pipe wall, and the connecting leads were purged of water using compressed air. Test flows at the throat had void fractions between 0.05 and 0.8, and the momentum flux parameter ranged from 0.05 to 0.10.

The observed variation of normalized pressure differentials over the contraction and test pipe sections are shown in figure 11(a) and (b). The sets of solid curves with constant void fraction and constant momentum flux parameter were calculated for certain ranges of void fraction and momentum flux parameter by a least-square polynomial fit, and the points indicate the observed results. Whilst figure 11 shows general agreement with figure 10 as predicted by the one-dimensional non-slip compressible flow model, it is clear that the experimental data actually show a rather better

spread of the measurement space than predicted. This is most likely due to slip and flow distribution effects which are not incorporated in the homogeneous flow representation, but it appears that such effects have enhanced rather than diminished the effectiveness of the metering principle. The enhancement is essentially reflected in a wider spread of the constant $D_0$ lines over the measurement space (figures 10 or 11) forming the basis for a more sensitive discrimination of both $D_0$ and $\epsilon_0$. The void fraction, momentum flux parameter, overall flow rate of water and overall flow rate of air, as predicted from the flow meter pressure differentials, are compared with values derived from externally measured water and air flow rates in detail in figure 12 for the abrupt contraction–pipe flow meter. Figure 13 shows the same comparisons for the conical contraction nozzle–pipe flow meter. The results shown in figures 12 and 13 incorporate the correction factors for the appropriate nozzle as discussed in section 2 ([9] and [10]) and for the pipe section friction factors (section 3, [16] and [17]). The maximum error between meter predictions and observations for liquid flow rate and momentum flux parameter is about 10% using the abrupt contraction–pipe flow meter. For

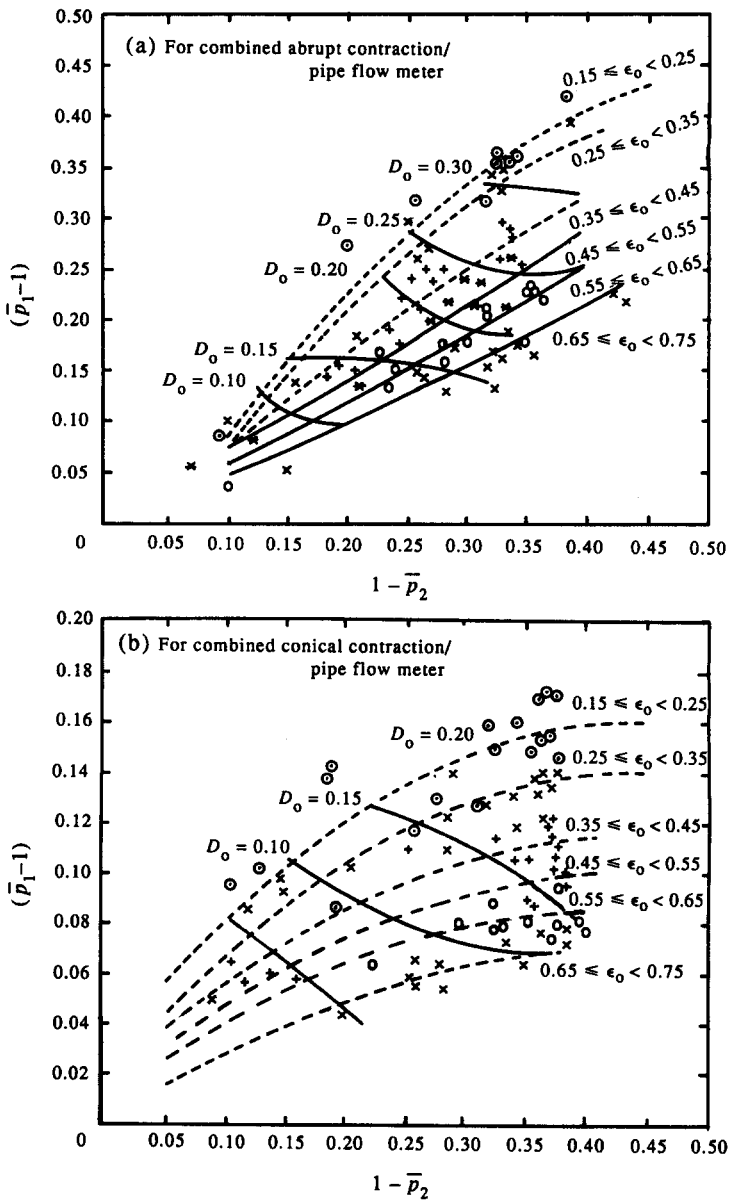


Figure 11. Observed variation of normalized pressure differential across a series contraction and a pipe. (a) For a combined abrupt contraction–pipe flow meter; (b) for a combined conical contraction–pipe flow meter.

void fraction and air flow rate, the points are more scattered and the maximum error between observed and predicted results for air flow rate is about 30% and about 20% for void fraction. According to the prediction model, the void fraction has much more influence on the wall friction factor of the pipe, whilst the momentum flux parameter $D_0$ has more effect on the velocity coefficient of the nozzle and is influenced in turn by the configuration of the contraction. Therefore, the scatter of predicted and observed air flow rate and void fraction will result mainly from the scatter of wall friction factor values with Reynolds number. More accurate prediction of air flow rate and void fraction using the dual pressure differential flow meter could be obtained by improving the correlation of wall friction factor with Reynolds number. In particular, the influence of void fraction on wall friction factor should be considered in detail. Also any measures which promote good inlet mixing and a flow pattern much closer to the homogeneous flow will improve the accuracy of metering. The points in figure 13 are seen to be more scattered than those in figure 12. This is most probably due to the effect of the flow pattern established in the contraction and pipe, since the abrupt contraction will promote stronger mixing and more homogeneous flow in the pipe section. It can be concluded that the configuration of the contraction not only influences

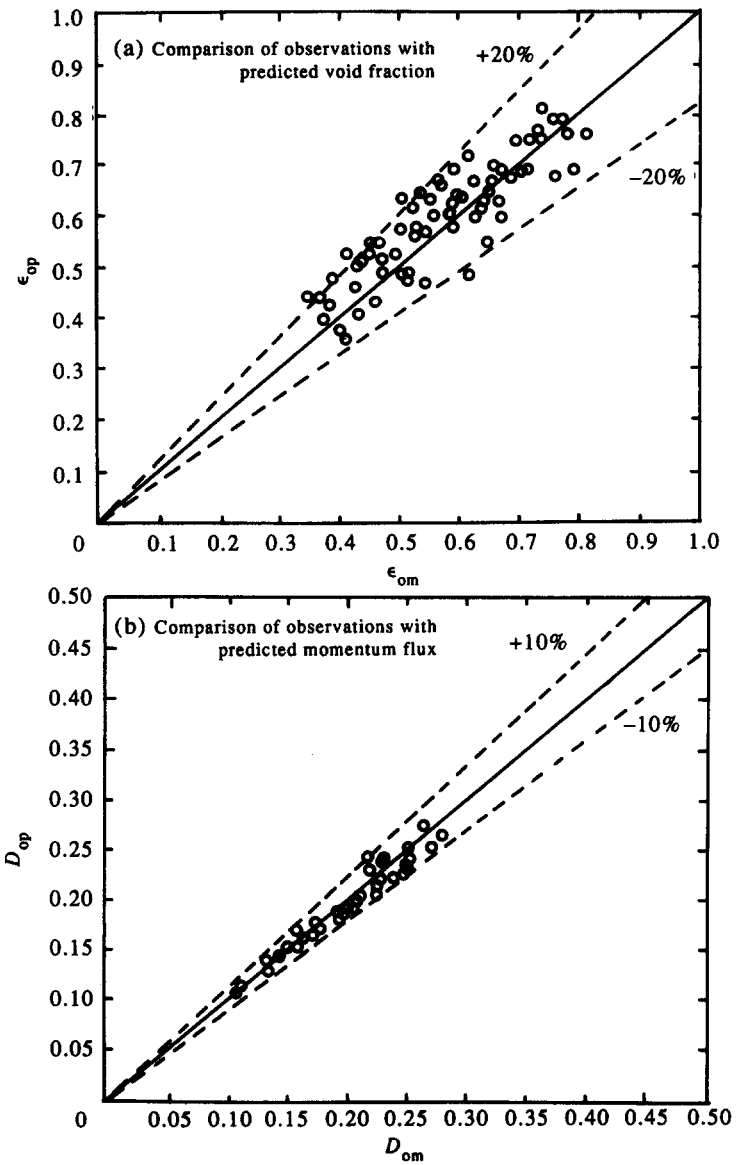


Fig. 12 (a) and (b). *Caption opposite.*

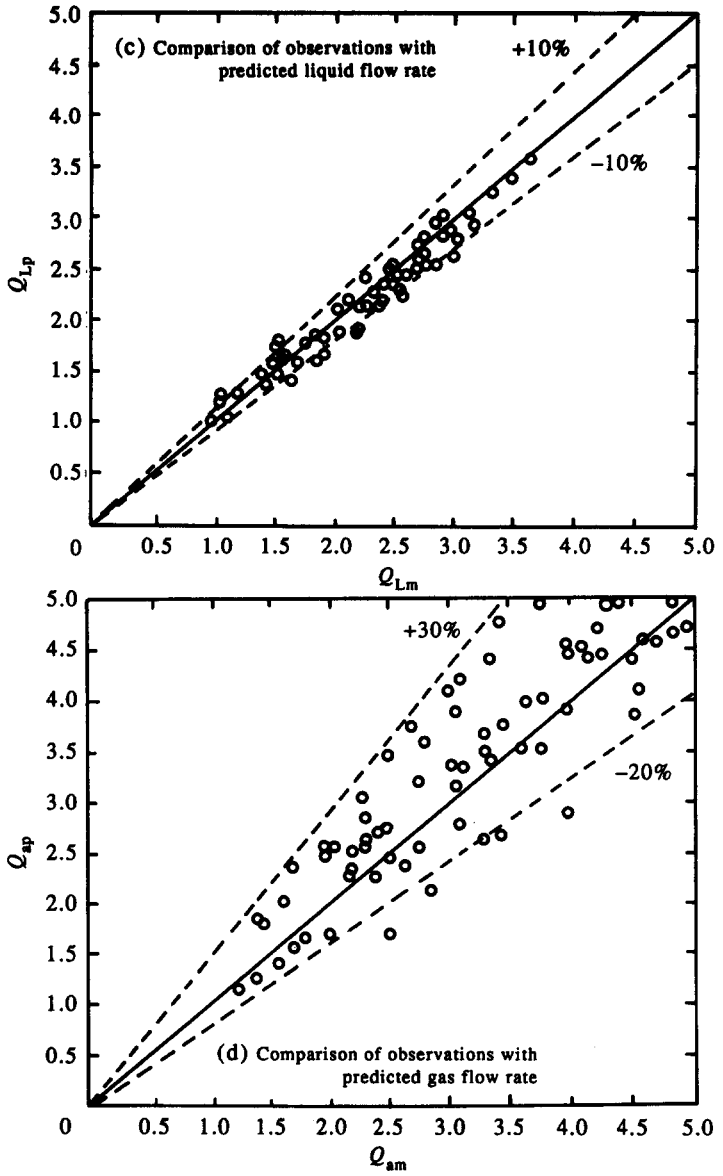


Fig. 12 (c) and (d)

Figure 12. Comparison of observed results with predicted results for a combined abrupt contraction–pipe flow meter. (a) Comparison of observations with predicted void fraction; (b) comparison of observations with predicted momentum flux; (c) comparison of observations with predicted liquid flow rate; (d) comparison of observations with predicted gas flow rate.

the pressure differential across the contraction itself, but also affects the accuracy of measurement in combined contraction–pipe flow meter. To improve the overall measurement accuracy, it would be better to adopt the abrupt contraction–pipe flow meter. This carries with it an increase in actual pressure loss across the contraction, but it appears that this effect is well-defined in terms of the nozzle velocity coefficient.

## 6. CONCLUSIONS

It has been shown that the combined use of a contraction in series with a frictional pipe flow section can form the basis for the measurement of both flow rates in a gas–liquid mixture flow from the observed pressure differentials over the two sections. An essential criterion for the operation

of such a metering device is that conditions of compressible flow should be established in the frictional pipe flow section so that sensitivity of the pressure drop in that section to void fraction and momentum flux is introduced. This depends on void fraction and momentum flux and corresponds to a requirement that the mixture momentum flux density at the pipe entry is approx. 0.3 of the pressure at that point if void fraction is less than 0.2. However, the conditions of choking at the pipe end should not be approached too closely, and the downstream pressure tapping should not be right at the pipe end to ensure this. Avoidance of the complexities of the choked end discharge would be ensured by locating the downstream tapping some 10 diameters at least ahead of the physical end of the pipe. The wall friction factor has a strong influence on the compressible flow characteristics especially for low values of momentum flux density at the pipe entry.

Experimental measurement in test contractions and pipe lengths show general conformity with the one-dimensional analysis for homogeneous bubbly flow conditions by taking into account the influence of the variation of pipe wall friction factor with Reynolds number and the velocity coefficient of the nozzle on void fraction. However, there is evidence that some variations of interphase slip occur and contribute to observed differentials. The configuration of the contraction

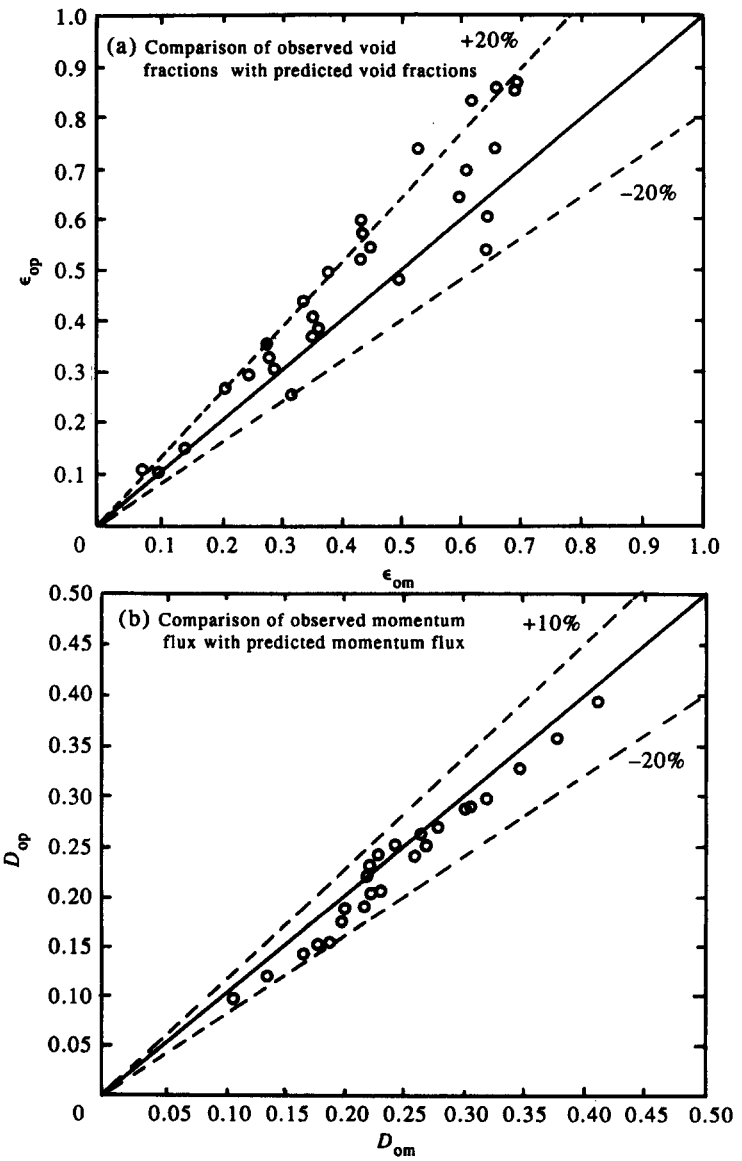


Fig. 13 (a) and (b). *Caption opposite.*

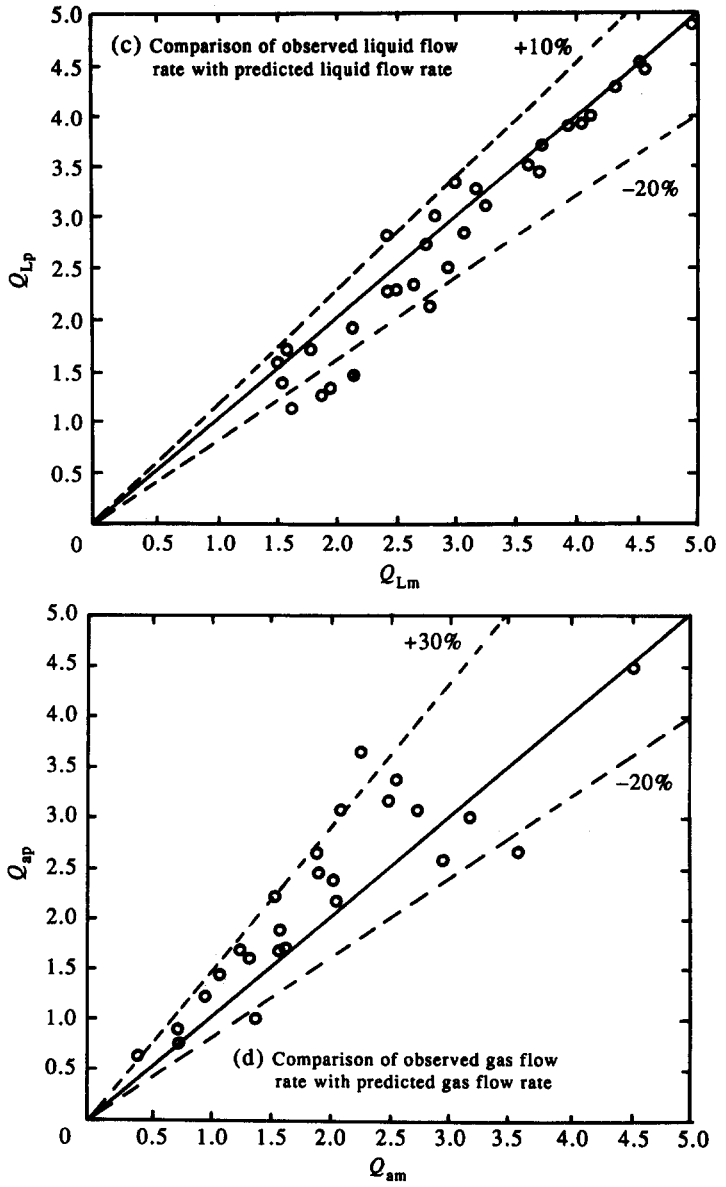


Fig. 13 (c) and (d)

Figure 13. Comparison of observed results with the results predicted by a real operation model for a combined conical contraction–pipe flow meter. (a) Comparison of observed void fractions with predicted void fractions; (b) comparison of observed momentum flux with predicted momentum flux; (c) comparison of observed liquid flow rate with predicted liquid flow rate; (d) comparison of observed gas flow rate with predicted gas flow rate.

also has an effect on the flow pattern in the compressible pipe flow, and will thus influence the wall friction factor of the pipe. It is likely therefore that it will be necessary to investigate these effects more closely in the context of specific combined flow meter designs, and to accommodate them through calibrations and corrections.

The normalized length $(x_2/d)$ of the frictional pipe section and the area ratio of the contraction can be varied over appreciable ranges without substantially influencing the compressible flow characteristics which make measurement of both phase flow rates possible. Whilst such flexibility exists in the selection of flow meter geometry, the design adopted will clearly influence the relative magnitudes of the two actual pressure drops which are to be measured to form the basis of the flow meter operation. The contour and area ratio of the contraction will also influence the flow

pattern at the pipe entry and through the frictional pipe section. Thus the configuration of the contraction has an influence on the friction factor in the frictional pipe section as well as on the pressure drop across the contraction. In order to improve the measurement accuracy, the abrupt contraction offers the best prospect of producing well mixed flows in the pipe section with minimal flow distribution and slip effects and consequently a more consistent and accurate overall performance. Whilst it is clear that the dual pressure drop flow metering principle is quite practicable, it will, in general, be necessary to calibrate such flow meters to allow for the detail effects of internal flow structure on their performance. A more extensive investigation of meter performance should offer a reasonable prospect of identifying the causes of data scatter and thus of improving the accuracy compared to that achieved in these initial trials. Also, voidage probe investigations would be necessary to determine whether the real flow effects (which depart from idealized homogeneous flow models) are due to voidage or velocity effects, or a combination of both.

The present paper has used the homogeneous flow model as a reference point to demonstrate the underlying basis of flow metering. It is clear that real flow effects must be incorporated through nozzle correction factors and pipe friction factors. However, it would be possible, of course, to adopt a simple nozzle calibration approach, relating the two flow rates to the two pressure drops. From a practical point of view this would be a more direct and workable means of real system calibration, but would not provide an underlying physical insight with regard to the basis of the metering method.

## REFERENCES

CAMPBELL, I. J. & PITCHER, A. S. 1958 Shock waves in a liquid containing gas bubbles. *Proc. R. Soc. A* **243,** 534–545.

COUET, B., BROWN, P. & HUNT, A. 1989 Two phase bubbly-droplet flow through a contraction: experiments with a unified model. *Proc. 10th Australasian Fluid Mechanics Conference*, University of Melbourne, pp. 7.29–7.32.

DAVIS, M. R. 1974 Determination of wall friction in vertical and horizontal two phase flow. *Trans. ASME J. Fluids Engng* **96,** 173–179.

DAVIS, M. R. 1991 Compressible gas–liquid mixture flow at abrupt pipe enlargements. *Exp. Thermal Fluid Sci.* **4,** 684–697.

HERRINGE, R. A. & DAVIS, M. R. 1976 Structural development of gas–liquid mixture flows. *J. Fluid Mech.* **73,** 97–123.

HERRINGE, R. A. & DAVIS, M. R. 1978 Flow structure and distribution effects in gas-liquid mixture flow. *Int. J. Multiphase Flow* **4,** 461–486.

HUEY, C. T. & BRYAN, R. A. A. 1967 Isothermal homogeneous two phase flow in horizontal pipes. *AIChE Jl* **13,** 70–77.

TANGREN, R. F., DODGE, C. H. & SEIFERT, H. S. 1949 Compressibility effects in two phase flow. *J. Appl. Phys.* **20,** 637–645.

THANG, N. T. & DAVIS, M. R. 1979 The structure of bubbly flow through venturis. *Int. J. Multiphase Flow* **5,** 17–37.

THANG, N. T. & DAVIS, M. R. 1981 Pressure distributions in bubbly flow through venturis. *Int. J. Multiphase Flow* **7,** 191–210.

VAN WIJNGAARDEN, L. 1970 On the structure of shock waves in liquid–bubble mixtures. *Appl. Sci. Res.* **22,** 366–381.